

PHYSICAL CHARACTERIZATION OF AN IMPACT VAPOR PLUME FROM A CHICXULUB CARBONATE LAYER USING LASER ABLATION IN A SIMULATED LATE CRETACEOUS ATMOSPHERE. K. F. Navarro^{1,2,3}, J. Urrutia-Fucugauchi², M. Villagran-Muniz⁴, C. Sánchez-Aké⁴, L. Perez-Cruz², and R. Navarro-González³, ¹Posgrado en Ciencias del Mar y Limnología, Universidad Nacional Autónoma de México (karis.navarro@nucleares.unam.mx), ²Programa Universitario de Perforaciones en Océanos y Continentes, Instituto de Geofísica, Universidad Nacional Autónoma de México, ³Laboratorio de Química de Plasmas y Estudios Planetarios, Instituto de Ciencias Nucleares, Universidad Nacional Autónoma de México, ⁴Laboratorio de Fotofísica y Películas Delgadas, Instituto de Ciencias Aplicadas y Tecnología, Universidad Nacional Autónoma de México.

Introduction: One of the major mass extinction events in the Earth's history occurred about 66 million years ago marking the Cretaceous–Paleogene (K-Pg) boundary [1, 2]. About 40% of the genera and 76% of the species went extinct in both continental and oceanic regions marking the end of the age of the dinosaurs and a turning point in biological evolution leading to the rise of mammals and birds [2-5]. Understanding the environmental changes that caused this event continues to be of great scientific interest [4, 6]. The leading hypothesis is an asteroid impact [2, 7-9]. Upon collision of the asteroid, a plume of fragmented, melted, and vaporized target rock expanded away from the impact site. The impact crater of the K-Pg event is found underneath the Yucatan platform, buried by up to 1 km of Cenozoic sediments [10, 11]. The crater, known as Chicxulub, is a multi-ring basin with semi-continuous, arcuate ring faults and a topographic peak-ring internal to the crater rim [12].

The purpose of this study was to characterize the spatial and temporal evolution of a simulated Chicxulub impact vapor plume using laser ablation of target sediments retrieved from the Yaxcopoil-1 borehole.

Experimental: The setup used to characterize the spatial and temporal evolution of the simulated Chicxulub impact vapor plume is shown in figure 1. The target material was a Cretaceous carbonate obtained at a depth of 980.13 m from the Yaxcopoil-1 drillhole cored ~60 km south-southwest of the center in the terrace zone of the southern crater rim of Chicxulub [13]. The chemical composition of the material was 86% of calcite (CaCO_3), 6% quartz (SiO_2), 6% palygorskite ($\text{Mg}\cdot\text{Al}_2\text{Si}_4\text{O}_{10}(\text{OH})\cdot 4(\text{H}_2\text{O})$), 1% halite (NaCl), and 1% sylvite (KCl) [14]. The simulated impact vapor plume was produced by focusing an intense pulse of radiation from a Nd:YAG laser operating at 1064 nm with a 7 ns pulse with an energy of 50 mJ on the Yaxcopoil-1 rock target with a repetition rate of 10 Hz. The ablation chamber was filled with a simulated late Cretaceous atmosphere composed of 0.16% CO_2 , 30% O_2 , and 69.84% N_2 at 1

bar and 25°C [14]. The atmosphere was prepared by mixing N_2 (99.998%), O_2 (99.99%) and CO_2 (99.8%) with a digital gas blending system operated with gas mass flow controllers.

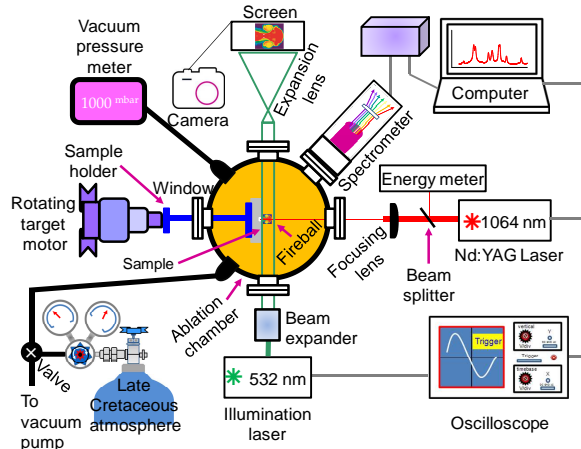


Fig. 1. Experimental setup to study the spatial and temporal evolution of a simulated Chicxulub impact vapor plume by shadowgraphy and emission spectroscopy.

The spatial evolution of the vapor plume was investigated by shadowgraphy. The ablated area was illuminated perpendicularly with an attenuated and expanded Nd:YAG laser operated at 532 nm. The images of the ablated plume were projected on a screen using an expansion lens, and were registered with a Nikon D70 commercial digital camera. The light emitted by the impact vapor plume was concentrated using a focusing lens located at ~5 cm from the ablation zone in front of one of the reactor windows at right angle to the direction of the laser beam, and sent with a fiber optics to a lens collector system. The spectrum was recorded with an intensified charged coupled device camera [14].

Results and Discussion. Figure 2 shows the shadowgrams obtained for the evolution of the impact vapor plume from 0 to 20 μs . The sudden release of energy by the laser pulse produced a small but strong explosion. The earliest images taken at $\leq 0.5 \mu\text{s}$ were indistinguishable from 0 μs because the shockwaves were hidden behind the target rock. It was only at $\geq 1 \mu\text{s}$ that the shockwaves became visible, and by 20 μs

they propagated beyond the field of view. The propagation velocity of the shockwave was calculated to be $4.5(\pm 0.1) \text{ km s}^{-1}$. The expansion of the simulated Chicxulub impact vapor plume was strongly decelerated by the formation of the shockwaves, and was visible from $2 \mu\text{s}$ with a hemispherical shape but then transformed into the typical so-called “mushroom cloud” by $20 \mu\text{s}$. The vapor plume propagated supersonically with an initial velocity of $2.3(\pm 0.4) \text{ km s}^{-1}$.

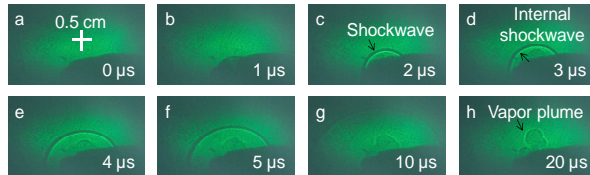


Fig. 2. Evolution of the shockwaves and impact vapor plume. The white cross indicates the scale of the viewing area; the black arrows point to the shockwave, internal shockwave and impact vapor plume.

Figure 3 shows the emission spectrum of the impact vapor plume at $1 \mu\text{s}$. Seventy spectral lines were identified corresponding to neutral as well as ionized atoms of calcium (Ca), magnesium (Mg), oxygen (O), nitrogen (N), and silicon (Si), and carbon (C) [14]. The emission spectrum was mostly populated by Ca, Ca^+ , O, and N lines. There were a few molecular bands detected that are very weak, and corresponded to the CaO orange system which indicated complete vaporization of the target material by the laser pulse.

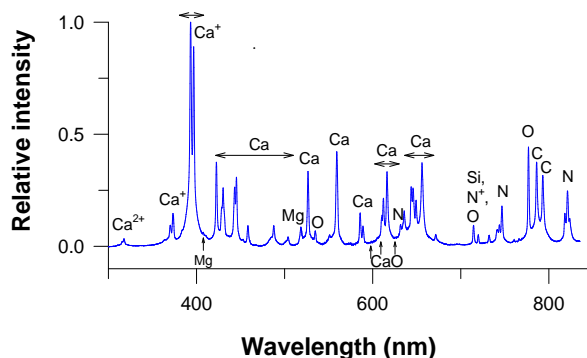


Fig. 3. Emission spectrum of the simulated Chicxulub impact vapor plume at $1 \mu\text{s}$.

Figure 4 shows the temporal evolution of the impact vapor plume as a function of electron number density (N_e), plasma temperature (T), and pressure (P). N_e was determined from the measured Stark broadened line profile using the Ca line at 649.965 nm . It was estimated to be $5.9(\pm 1.1) \times 10^{17} \text{ particles cm}^{-3}$ at $0.2 \mu\text{s}$ and dropped to $4.0(\pm 0.4) \times 10^{16} \text{ particles cm}^{-3}$ at $4.2 \mu\text{s}$.

T was determined by the Saha-Boltzmann plot technique using emission spectroscopy with deconvolution spectra for two singly ionized and ten atomic Ca lines. It was estimated to be $1.8(\pm 0.1) \times 10^4 \text{ K}$ at $0.2 \mu\text{s}$ and dropped to $6.9(\pm 0.2) \times 10^3 \text{ K}$ at $4.2 \mu\text{s}$. P was estimated to be $103 \pm 1 \text{ bar}$ at the start of the shockwave assuming adiabatic expansion of a hemispherical plume [15]. At later times P was computed using T and N_e with the ideal gas equation of state [16]. It was estimated to be $3.0 \pm 0.2 \text{ bar}$ at $0.2 \mu\text{s}$ and dropped to $0.1 \pm 0.01 \text{ bar}$ at $4.2 \mu\text{s}$.

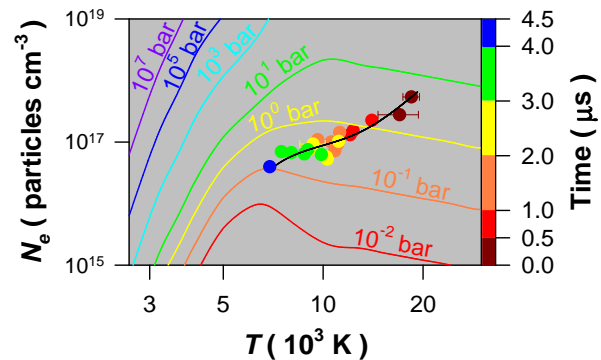


Fig. 4. Temporal evolution of the simulated impact vapor plume as a function of T , N_e and P .

The physical and chemical parameters derived in this study are important for future studies to predict the evolution of chemical species and mineral phases that originated by the Chicxulub impact vapor plume. Such models will enable to better understand the chemical effects of the asteroid impact to the environment and the biosphere.

Acknowledgments: We acknowledge UNAM (PAPIIT IN11619 and PAPIIME PE102319) for financial support.

References: [1] Renne, P.R. et al. (2013) *Science*, 339, 684–687. [2] Schulte, P. et al. (2010) *Science*, 327, 1214–1218. [3] Bambach, R.K. (2006) *Annu Rev Earth Planet Sci*, 34, 127–155. [4] Brusatte, S.L. et al. (2015) *Biol Rev*, 90, 628–642. [5] Wilf, P. and Johnson, K.R. (2004) *Paleobio*, 30, 347–368. [6] Prauss, M.L. (2009) *Palaeogeogr Palaeoclimatol Palaeoecol*, 283, 195–215. [7] Alvarez, L.W. et al. (1980) *Science*, 208, 1095–1108. [8] Gulick, S.P.S. et al. (2019) *Proc Natl Acad Sci USA*, 116, 19342–19351. [9] Hull, P.M. et al. (2020) *Science*, 367, 266–272. [10] Hildebrand, A.R. et al. (1991) *Geology*, 19, 867–871. [11] Paull, C.K. et al. (2014) *Mar Geol*, 357, 392–400. [12] Gulick, S.P.S. et al. (2013) *Rev Geophys*, 51, 31–52. [13] Urrutia-Fucugauchi, J. et al. (2004) *Meteorit Planet Sci*, 39, 787–790. [14] Navarro, K.F. et al. (2020) *Icarus*, 346, 113813. [15] Zeldovich, Y.B. and Raizer, Y.P. (1966) *Physics of Shock Waves and High-Temperature Hydrodynamic Phenomena*, Academic Press, London. [16] Kurosawa, K. and Sugita, S. (2010) *J Geophys Res Planets*, 115, E10003.